Formation and Growth Mechanism of Dissimilar Coiled Carbon Nanotubes by Reduced-Pressure Catalytic Chemical Vapor Deposition

Mei Lu and Hu-Lin Li*

Department of Chemistry, Lanzhou University, Lanzhou, 730000 China

Kin-Tak Lau

Department of Mechanical Engineering, The Hong Kong Polytechnic University, Hung Hom, Kowloon, Hong Kong, China

Received: July 14, 2003; In Final Form: January 21, 2004

Dissimilar coiled carbon nanotubes were prepared by catalytic chemical vapor deposition (CCVD) on finely divided Co nanoparticles supported on silica gel under reduced pressure and at lower gas flow rates. The morphology of the regular coiled carbon nanotubes were examined by TEM, while the polygonization characteristics of the helix were examined by SAED. Observations were made on other forms of irregular coils with various shapes by TEM. On the basis of the heptagon−pentagon construction theory, we proposed a helix formation mechanism, which involves a carbon core formation centering on a catalytic particle followed by carbon helices growth controlled by kinetics.

1. Introduction

Since the discovery of carbon nanotubes (CNTs) by Iijima in 1991, extensive research has been carried out to investigate the electronic, physical, and mechanical properties of novel materials. Research results have shown that CNTs with various shapes, such as straight,[1] curved,[2] coiled,[3] and bamboo-shaped,[4] each have their own unique characteristics and potential applications. Specifically, the helical structure of regular coiled nanotubes has been found to have far superior mechanical stability in addition to its prominent attribute of being able to cross-polarize electromagnetic waves. By anchoring in an embedding matrix with mechanical interlocking, regular coiled nanotubes improve the overall strength and toughness of composites under axial, torsional, bend, and other types of forces frequently seen in nature.[5,6] Recent reports indicate a high Young's modulus around 0.17 TPa has been measured for the coiled nanotubes by atomic force microscope (AFM).[7] In addition, the ability of coiled CNTs to cross-polarize electromagnetic waves, when combined with its natural light-mass and low-reflection property, means that CNTs could be an attractive novel material for high-performance microwave absorption.[8,9] For these two reasons, having a reliable and efficient method for obtaining regular coiled nanotubes is an important issue for both experimental and future application usage.

Among many published techniques for the fabrication of CNTs, catalytic chemical vapor deposition (CCVD), carried out with a small quartz tube under atmospheric pressure and high gas flow rate, has been found to be the only reliable method that can produce helical nanotubes with fine regular coils.[10] However, the drawback with this approach is with the low yield of coiled CNTs on the basis of required high gas flow rate for the deposition. In the normal CCVD process, a high percentage of the gases used (such as C_2H_2, H_2, and N_2) are discharged into the atmosphere without any participation in the chemical reaction. As such, this process is not suitable for the scaled-up production of coiled CNTs. The consumption of hydrocarbons such as acetylene under high pressure in the production process would cause major safety concerns. In addition, the inefficiency in the use of the gases would likely raise environmental issues. Therefore, it is desired to explore a more efficient, secure, yet still reliable CCVD method for the growth of coiled nanotubes.

In the work presented, coiled CNTs are produced by CCVD acetylene on finely divided Co nanoparticles supported on silica at reduced pressure and lower gas flow rates. The substantial reduction in the consumption of C_2H_2 under the described reaction condition greatly alleviates environmental concerns as well as safety issues associated with traditional CCVD methods. The goal of this paper is to investigate the formation of coiled carbon nanotubes produced in reduced-pressure conditions using TEM, providing some helpful fundamental theories and practices for the scaled production. In section 3.1, the morphologies of dissimilar coiled nanotubes were examined by TEM; in section 3.2, SAED and HRTEM were employed to study the crystallization of the regular coiled nanotubes; in section 3.3, the growth mechanism for the coiled carbon nanotubes via core formation followed by helix continuum was discussed.

2. Experimental Section

The cobalt catalyst supported on silicagel H(5−40 μm) was prepared by pH-controlled ion-adsorption precipitation.[11] A 0.6 g quantity of cobalt acetate [$Co(CH_3COO)_2 \cdot 4H_2O$]] was dissolved in 50 mL of distilled water. The pH of cobalt acetate solution was controlled using liquid ammonia with pH-indicator strips checking. A 1-g quantity of silicagel support was added to the cobalt solution and allowed to sonicate for 4 h. The prepared catalyst was then dried in air overnight at 100 °C. The catalyst took on an olive color after drying. The dried catalyst was then ground to the form of a fine powder for subsequent deposition.

The catalysts were placed in a cylindrical quartz boat positioned in the center of a quartz tube placed within a

* Corresponding author. E-mail: lihl@lzu.edu.cn.

10.1021/jp0360265 CCC: $27.50
Published on Web 04/24/2004

SCHEME 1: Coiled Carbon Nanotube with Its Projection (right) Showing the Coil Diameter and Coil Pitch

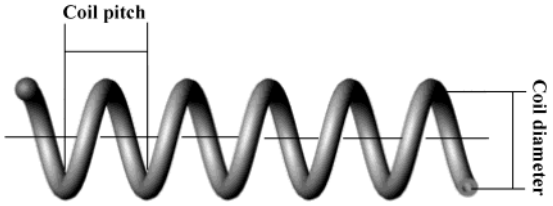

horizontal tubular electric furnace. The reactor was then evacuated to a base pressure of 100 Pa with a mechanical pump. After the reactor was heated to 720 °C at a rate of 15 °C/min, acetylene gas (C_2H_2) of 20 sccm was flowed into the reactor for 30 min. The final product was then purified as follows: cobalt particles were removed by immersion into a 30% HNO_3 solution under sonication for 30 min and the solution was allowed to settle for 4 h, followed by rinsing with distilled water using filtration; the silicagel support was separated via sonication in an organic solvent mixture (*n*-heptane/acetone/2-propanol = 1:1:1) and then rinsed with distilled water with filtration.

All purified nanotubes produced at pH values of 7.5, 8.5, and 9.5 were sonicated at low power in alcohol and dropped onto a piece of holey carbon grid. Conventional transmission electron microscope (TEM) and high-resolution TEM analyses were both performed on a JEOL-2010 microscope at an acceleration voltage of 200 kV.

3. Results and Discussion

3.1. TEM Analysis. The geometrical parameters of the coiled carbon nanotubes are illustrated in Scheme 1. A longest coiled nanotube, like a stretched miniature telephone cord, with a length of 5.5 mm is shown in Figure 1. It has a remarkable constant coil pitch and a diameter of 67 and 40 nm, respectively.

The regular coils in the same sample can take on varying degrees of tube diameters, coil diameters, and coil pitches. Figure 2a shows coiled nanotubes with tube diameter of ~35 nm but with much different coil morphology. These coils have different coil pitches, such as slightly curved tubes, weakly coiled spirals and spring-like forms. Other coiled tubes of 15 nm diameter with a wavy appearance and braided together are also observed, but are considered as accidental and are also shown in Figure 2b. Among the various coiled formations, a good portion of them are highly compressed coiled nanotubes (Figure 2c). The appearances of regular circles of bright spots are the tube sections of the nodes formation, due to the very small coil pitch of this particular type of nanotubes. Another observed coil shape is the loop-wire shaped nanotubes (as shown in Figure 2d), which are formed with periodic curvature and knots during the growth of nanotubes. Unlike double-twisted micro-coiled carbon fibers,[12] coiled nanotubes are generally of single coils and, more importantly, are hollow in the center.

Most of the helical tubes are coiled in a regular fashion with a constant curvature, suggesting that the growth rate of the tube in the axial direction is much faster than that in the radial direction. However, industrial acetylene always contains a very low concentration of a sulfur compound, which is a very strong poison for Fe, Co, and Ni catalysts.[13] Apparently, the activity of a Co catalyst and a number of active sites may be reduced due to the very strong interaction existing between the sulfur compound and the active sites in the Co particles. Therefore the resulting tubulars may be of complicated shapes because of the change of the catalyst activity caused by the local poisoning.

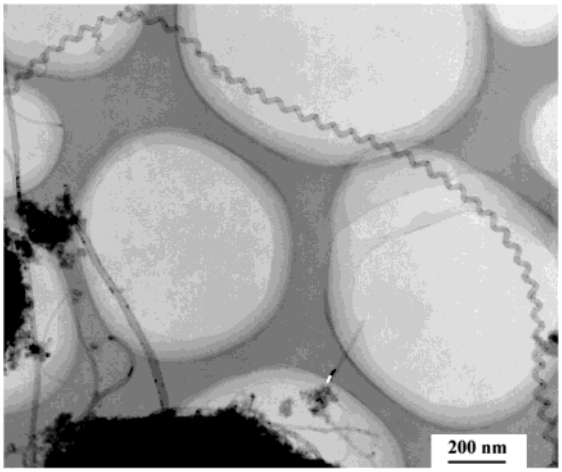

Figure 1. The longest coiled carbon nanotube with regular pitch found in our experiment (pH = 8.5).

In the case of only slightly coiled tubes with pitches in the 200 nm range (Figure 3a), most of the tube clearly exhibits typical graphitic structure with an inter-planar spacing of 0.34 nm. The inner layers of the tube with an imbricated structure display dislocation or local buckling of the planes, while the outer graphitic sheets have a relatively constant curvature. Figure 3b shows that the diameter of the coil core is often irregular, with frequent constrictions or expansions during growth. At an atomic scale, these observations appear to be due to the buckling of the graphite planes or lattice defects structures. At times, under rare but undetermined conditions, coiled nanotube growth could be random, as is what occurred in the case of Figure 3c. The curved segment in the middle and two coiling parts at the both ends coexist on the same body of the nanotube. The periodicity of the coiling also varies along the helical structures. Another interesting type of observed coil growth occurred in a planar-spiral fashion. The location of catalytic particle shown in Figure 3d provides evidence that nanotube growth follows along the direction of decreasing coil diameter gradually, eventually terminating with the formation of a snail-like helicoid. Figure 3e shows that an in-planar spiral can coil forward in different planes with inter-planar distances as large as ~230 nm, with a conic spring pattern. If the variance between the coil diameters is not too large, the spiral could extend to as many as five revolutions (Figure 3f).

To determine the distribution of the parameters of coiled nanotubes under different experimental conditions, the dimensions of a large number of tubes on TEM holey carbon grid samples are measured. The parameters distribution histogram for the coiled nanotubes prepared at pH = 8.5, such as inner diameter, outer diameter, coil pitch, and coil diameter, is diagrammed in Figure 4a and b. As shown in Figure 4a, the distribution of the inner diameters is narrow and in the range of 2.3−6 nm with an average of 4.5 nm. The outer diameter distribution is wider and in the range of 3−20 nm with an average of 12 nm. Overall coil pitches and coil diameters fall in the ranges from 10 to 220 nm and 10−100 nm, respectively. For coiled nanotubes, those with larger coil diameters can easily be stretched to 6−10 times that of the original coiled length; therefore, it is within reason to expect that good elasticity may exist in these specially shaped carbon nanotubes.

3.2. SAED and HRTEM Analysis. The selected area electron diffraction (SAED) pattern for several turns of the helix in a coiled nanotube is shown in Figure 5a, which consists of two continuous arcs with an angular width $2\theta = 68°$. On the basis of geometrical analysis of the electron diffraction, the

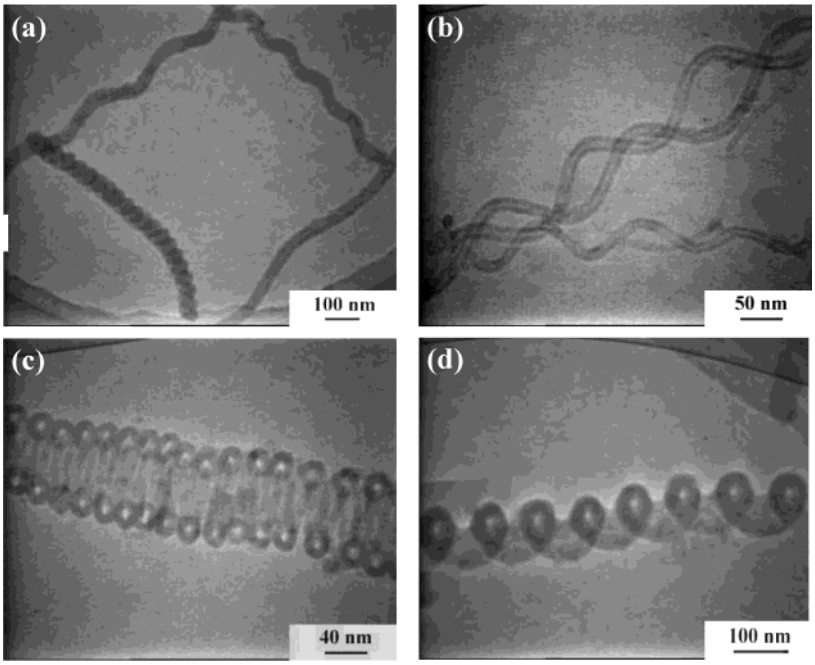

Figure 2. (a) Four coils with various pitch and diameter; (b) several wavy nanotubes twisted with each other; (c) highly compressed coiled nanotubes with nodes; (d) loop wire shaped nanotube. (All these coils were produced at pH = 9.5).

indices of the diffraction rings are demarcated in the image. When the selected area only covers one turn of the helix in a coiled nanotube (Figure 5b), the arcs becomes "spotty" with an angular width $2\theta = 120°$, exhibiting a larger dot intensity at the extremities than that at the center parts. This indicates that the smaller the selected area, the clearer the crystallization in the SAED pattern. The SAED result suggests that the curvature is not continuous in microscale but that the helix consists of short straight segments, i.e., the helix is polygonized. This conclusion can also be derived from high-resolution TEM images as discussed below.

Graphitization of a short straight section in a regular coil shown in Figure 6a was observed by HRTEM. Figure 6b shows that the straight segment in the regular coil actually consists of concentric graphitic sheets with a spacing of 0.34 nm, contrasting this with the well-known micro-coiled carbon fibers that usually consist of amorphous carbon fibers. Although the curvature appears to be continuous segments at low magnification, the HRTEM images show that the regularity in the coils on a micrometer scale does not correspond to a perfect periodic repetition of the atomic structures. Detailed examination of one of the periodic bends (Figure 6c) shows that part of the nanotube displays clear graphitic layers. However, the places where there is buckling to achieve the angle compatible with the coil periodicity are not perfect. Therefore, the true periodicity must be determined at a much larger scale. In this image, there are other parts of the coil that are not clearly resolved, attributed to the 3D-shape of the helix and the limited depth of focus in the TEM (typically ~10 nm).

To make a clear observation on the microstructures of the node for highly compressed coiled nanotubes, a node directly facing (pointing to) the lens of the camera was chosen for ease of analysis with phenomenon HRTEM recording. As shown in Figure 7, a circular lighter region is at the center of the node, around which the graphitic layers circulate with an inter-planar spacing of 0.34 nm.

On the basis of observations at the coil ends whenever possible, catalyst particles generally appear to be located at the bottom of the tube, indicating that the growth proceeds from the base at metallic particles dispersed on the supports. The catalyst particles can take various shapes, such as circular, slightly elliptical, and elongated grain as shown in Figure 8. It is also noted that most of the tubes are closed at their ends. Only in rare cases are they seen open at one of their ends. The growth process for the open-ended tubes seems to have been terminated at the ends by some sudden change in the growth conditions.

3.3. Growth Mechanism of the Coiled Carbon Nanotubes. To date, several growth mechanisms have been proposed for the carbon coil formation. Fonseca et al.[14,15] suggested a growth mechanism on a catalyst particle at a molecular level using the heptagon−pentagon construction of Dunlop[16] and explained the formation of curved nanotubes, tori, or coils. On the basis of the concept of a spatial-velocity hodograph, Amelincks et al. proposed a growth mechanism for the carbon nanocoils.[3] It is concluded that the mismatch between the extrusion velocities of carbon from the catalyst grain results in the helix. By deriving a string action expression for the formation energy of the multiwalled CNTs as well as its equilibrium-shape equation, Ou-Yang et al. found straight nanotubes will become unstable and regular coiled nanotubes may be formed below a threshold condition.[17] Seiji Motojima postulated a 3D-growth mechanism of carbon coils based on the "anisotropy of carbon deposition" theory, which relies on an assumption that the different catalytic activities of the crystallographic facets define the geometry of the CNTs.[18]

On the basis of the HRTEM images shown in Figures 8 and 9, we believe the coil growth process involves a core cluster formation and then a helical tube formation. Pentagonal, hexagonal, and heptagonal carbon rings play important roles in the growth of the coiled tubes. As indicated in Scheme 2, the hexagonal carbon rings are the basic structural units that form the graphites lattices. The nucleation of pentagons (+60° disclination) at the periphery of the open ends of growing tubes induces closure of the tubes. Heptagons (−60°), in contrast, can reverse the cone shape to cylindrical and annul the effect of pentagons.[19] In either case, the nucleation of pentagons and heptagons changes the direction of growth in a growing tubule

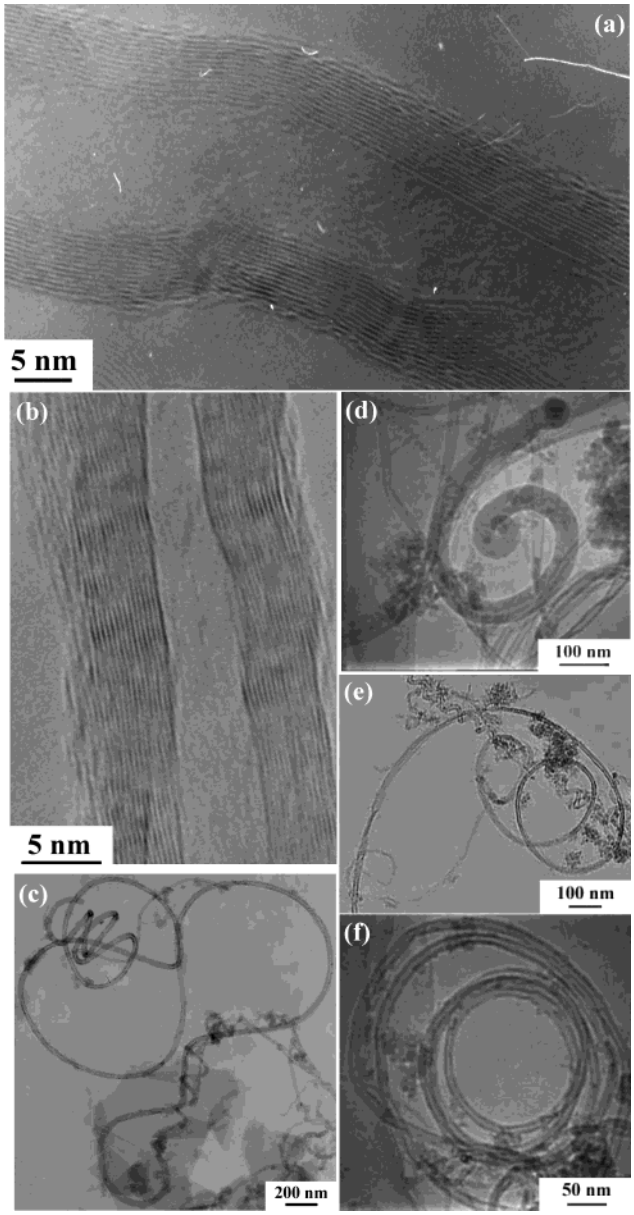

Figure 3. (a) HRTEM image of the curvature in a slightly coiled nanotube (pH = 7.5). (b) HRTEM image of a coiled nanotube with varying diameter (pH = 7.5). (c) TEM image of a nanotube with helical part coexisted with curved part (pH = 9.5). (d) TEM image of a snail-like nanotube (pH = 9.5). (e) TEM image of a conic spring-like nanotube (pH = 8.5). (f) TEM image of a planar-spiral nanotube with five revolutions (pH = 8.5).

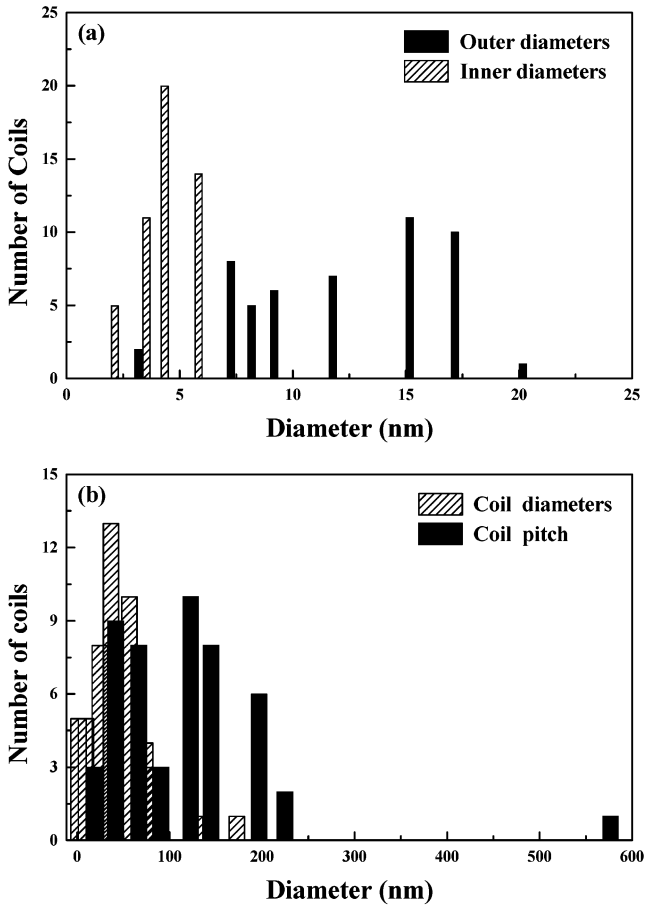

Figure 4. Inner diameter, outer diameter (a), coil diameter and coil pitch (b) distribution histograms of coiled nanotubes produced at pH = 8.5.

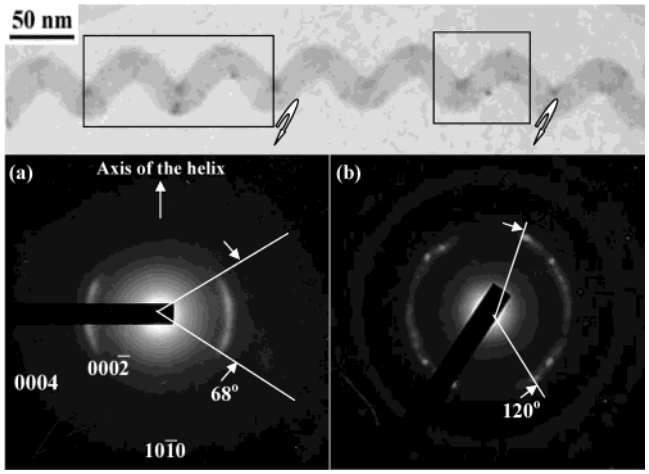

Figure 5. Selected area electron diffraction (SAED) patterns corresponding to the area selected by the left (a) and right rectangle (b) in a coiled nanotube (pH = 8.5).

by introducing curvature. That is to say, a zero-curved surface is created by the nucleation of hexagonal carbon rings, a positively curved surface is created by insertion of pentagons into a hexagonal sheet, and a negatively curved surface is created by insertion of pentagons. By combining the two surfaces appropriately, in principle, different types of toroidal carbon forms with quite interesting geometrical properties could be formed, such as C_{360}, C_{540}, and C_{576}.[16]

With these basic concepts in mind, the coil formation mechanism in our case could be explained. It should involve two steps: (1) the formation of a carbon core cluster, and (2) the continuous growth of a helical nanotube. The catalyst particle serves as a nucleation center to dissolve the gaseous carbon atoms decomposed from C_2H_2. Oversaturation will result in an extrusion of solid carbon from one surface of the catalyst particle. Due to the changes of experimental conditions and the inhomogeneous catalytic activity in the particle, the extrusion speed can therefore be complicated and may, for instance, create a pentagonal carbon ring in random (Scheme 3a), which is the start of the spiral-shell growth model. If a few pentagonal carbon rings are introduced in the graphite lattice, a quasi-icosahedral spiral shell with a catalytic particle encapsulated at the center can be shaped (Scheme 3b), but this core-shell structure is unclosed in order to continuously grow into a large particle with pentagonal carbon rings supplied continuously[20] (Scheme 3c). However, if no pentagonal carbon rings are created for a very

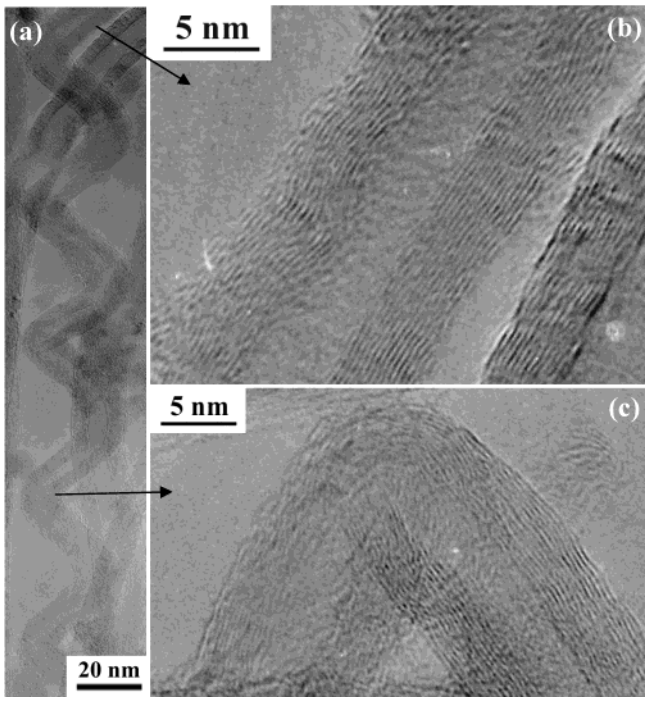

Figure 6. (a) TEM image of a coiled nanotube (pH = 8.5), (b) HRTEM image recorded from a straight section in the coil, and (c) HRTEM image recorded from a bend in the coil.

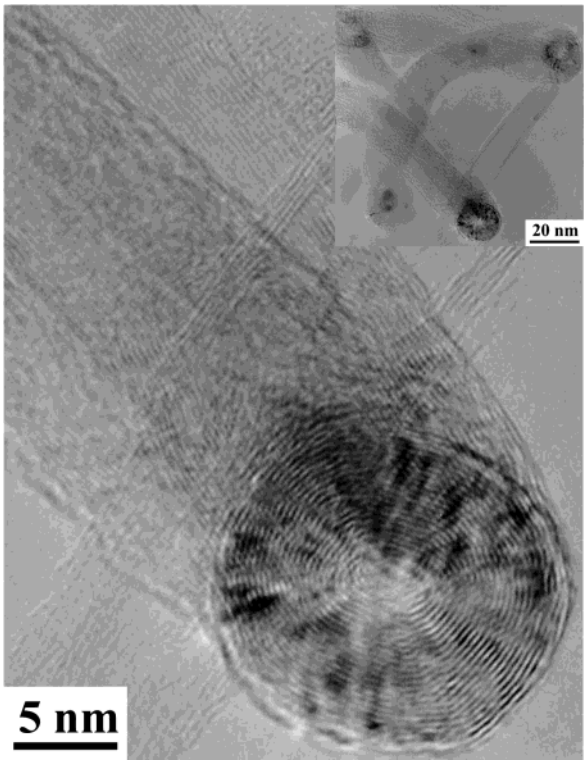

Figure 7. HRTEM image of a node in a coiled nanotube (inset shows the coil morphology at lower magnification).

short period of time and the hexagonal carbon rings are continuously supplied, the spiral layer will grow outward, forming a tube structure (Scheme 3d), and its subsequent growth would be the same as that of a straight carbon nanotube. It seems as if the core-shell structure is used as the base for the growth of a nanotube.

Detailed TEM analysis (Figure 8) shows that almost all of the catalyst particles are completely surrounded by carbon shells,

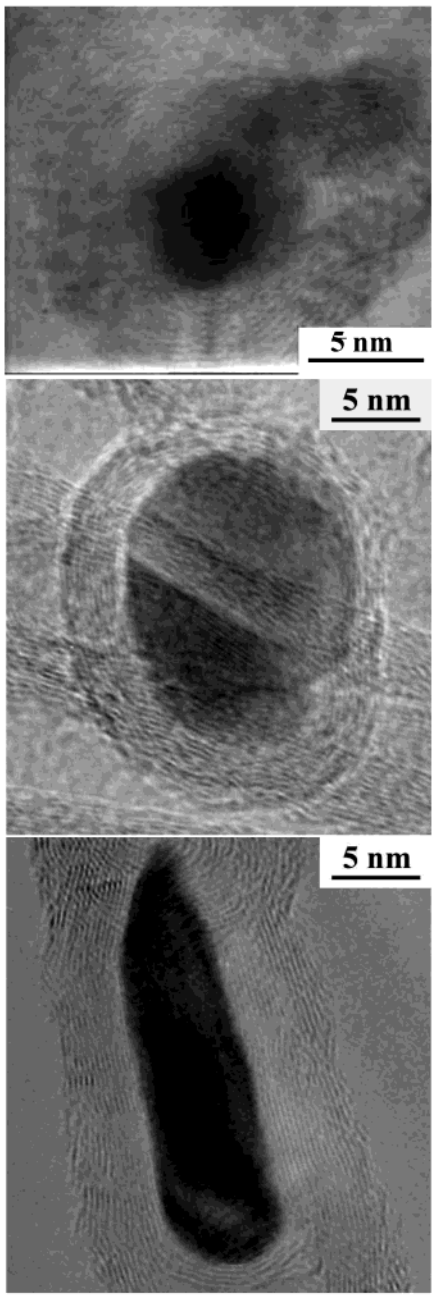

Figure 8. Typical HRTEM images of the catalyst particles encapsulated by graphitic shells.

indicating that the catalyst particles were initially involved in the nucleation of the carbon tubes, but they may not be directly involved in the entire life of coil growth, due to the termination of catalytic activity. Since the nucleation of pentagons and heptagons can change the direction of growth by introducing curvature, the following growth of thehelix should be determined by the creation rate of the periodic production of pentagon−heptagon-pair dislocations (PHPDs) in diametrically opposite parts of the tube. Furthermore, in the midst of the nanotube with hexagonal network growth, if a PHPD is created, the tube will be forced to twist, for example, clockwise (Scheme 3e). Another twist is introduced if a second PHPD is introduced. The number of PHPDs determines the total twist angle. The periodical distribution of PHPDs through the entire growth process possibly results in the periodically distributed nodes or curvatures. If the orientation of PHPDs rotates along the body of the tube, a helical tube would be produced (Scheme 3f).

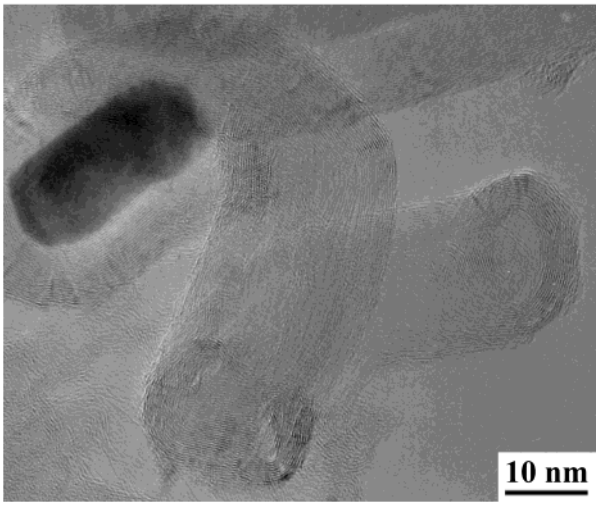

Figure 9. HRTEM image of a section of coiled nanotube with a catalyst particle, indicating the growth mechanism.

Accordingly, the major driving force for the different coil formations is the creation rate of the PHPDs, which can determine geometrical parameters, such as the twist angle, coil pitch, and coil diameter. This is a kinetically controlled growth process.

In practice, the nucleation rate of carbon rings can vary according to the fluctuation of experimental conditions, such as reaction pressure, temperature, and gas flow rate, as well as some uncertain factors. The continuous growth of the helix tubes requires a continuous supply of PHPDs and a constant creation rate of the PHPDs in order to maintain the coiled shape. If no PHPD is supplied in a period (the creation rate ofPHPDs is zero), a straight section of the tube could be produced, which is in agreement with the observation shown in Figure 9c. If the creation rate of PHPDs is very slow and the PHPDs are distributed periodically, a slightly curved nanotube would be formed. If the creation rate of PHPDs is very fast and the interpair distance is very small, a highly compressed coiled nanotube with circular nodes would be formed, as shown in Figure 2c. If the creation rate of the PHPDs is fluctuant, the coiled tubes with irregular coil diameter and coil pitch could be produced. If the orientations of the PHPDs are in the same plane, a planar-spiral structured nanotube would be formed, in which the creation rate of the PHPDs can determine the planar-spiral structure with or without the same coil diameter.[15]

Although the creation rate of PHPDs can determine the geometrical parameters of the coiled nanotubes to a certain extent, the creation rate of PHPDs could not be finely controlled to selectively grow coiled nanotubes with a particular shape or with a constant coil pitch in the same sample thus far. This is because the creation rate of PHPDs carbon rings may depend on the fluctuation of the experimental conditions during the carbon ring nucleation and other factors that warrant further study.

The one question that remains is why the PHPDs appear periodically rather than randomly to form the helical structure? Dunlap pointed out that this regularity could be caused by the defect−defect interactions and constraints on the optimal heptagon−pentagon nanotube bend.[16] On the other hand, if the pentagonal and heptagonal rings are not regarded as defects, but as regular building blocks, then their very precise positioning may be regarded as an inherent property of the structure. According to theoretical calculations, CNTs built from regular pentagons and heptagons pairs, named Haeckelite tubes, are energetically more stable than C_{60}.[21] This finding is in agreement with experimental observations, which shows that coiled nanotubes are not attacked during wet oxidation despite containing a large number of nonhexagonal rings.[22] By taking account of competition among the curvature elasticity, the adhesion of outer and inner surface of CNTs (the sum of these three energies can

SCHEME 2: (a) Hexagonal, (b) Pentagonal, (c) Heptagonal Carbon Ring Structures in Graphitic Sheets

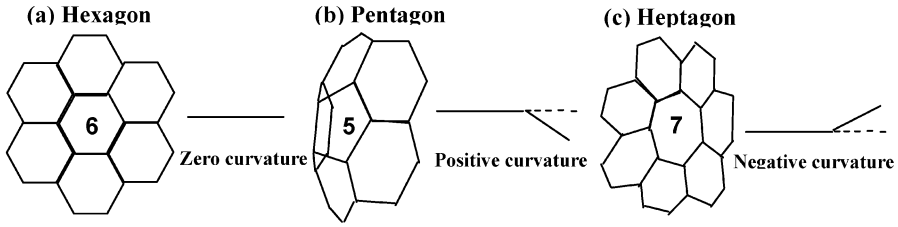

SCHEME 3: (a) Nucleation of a Pentagon, (b) Growth of a Quasi-icosahedral Shell, (c) Formation of a Spiral Shell Carbon Encapsulated Catalyst Particle, (d) Growth of a Straight Carbon Nanotube, (e) Formation of a Node along the Straight Carbon Nanotube, and (f) Formation of a Coiled Nanotube

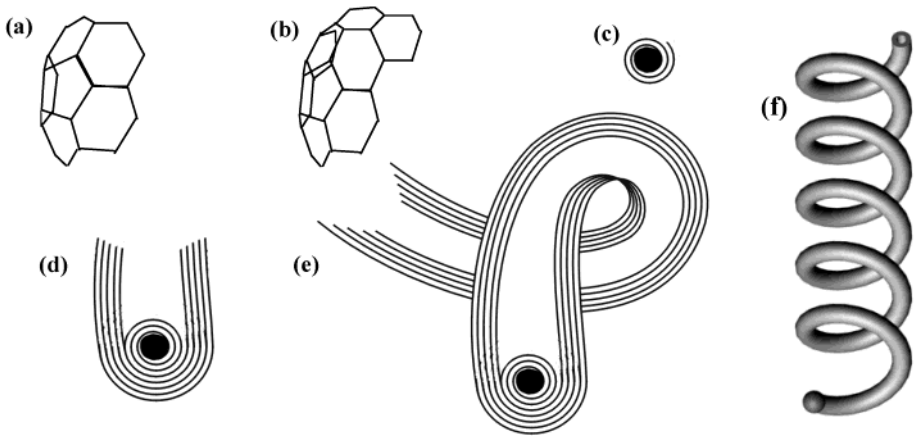

be understood as the shape formation energy), the formation of regular coils was shown to correspond to an energy-minimum shape as well as that of the straight tube. An optimal conditions pitch/coil diameter $= 2\pi$ for the regular coils could be derived.[16] Accordingly, the coiling of the nanotube may be attributed to an abrupt release of bond strain.

4. Conclusions

Coiled carbon nanotubes have been prepared by catalytic chemical vapor deposition (CVD) on silica-supported Co nanoparticles under reduced pressure and at lower gas flow rates. TEM results indicate that the regular coiled carbon nanotubes displaying different morphologies, such as slightly curved, spring-like formed, highly compressed coiled, and loop-wire shaped nanotubes, etc. Other forms of irregular coils with various shapes were also observed by TEM. The distributions of the inner diameters and outer diameters are in the range of 2.3−6 nm and 3−20 nm, respectively. The coil pitches fall in the range of 10−220 nm and coil diameters in the range of 10−100 nm. The SAED result suggests that the helix is polygonized, which is further confirmed by HRTEM images recorded from the coil tube, coil bend, and coil node. On the basis of the heptagon−pentagon construction theory, the helix formation mechanism that involves a carbon core formation centering on a catalytic particle followed by carbon helices growth controlled by kinetics is proposed.

Acknowledgment. This project was supported by the National Natural Science Foundation of China (G-60171004) and the Hong Kong Polytechnic University Grant (G-T684).

References and Notes

(1) Ebbesen, T. W.; Ajayan, P. M. *Nature* **1992**, *358*, 220.
(2) Martel, R.; Shea, H. R.; Avouris, P. *Nature* **1999**, *398*, 299.
(3) Amelinckx, S.; Zhang, X. B.; Bernaerts, D.; Zhang, X. F.; Ivanov, V.; Nagy, J. B. *Science* **1994**, *265*, 635.
(4) Louchev, O. A. *Phys. Status Solidi A* **2002**, *193*, 585.
(5) Hayashida, T.; Pan, L.; Nakayama, Y. *Physics B* **2002**, *323*, 352.
(6) Lau, K. T.; Li, H. L.; Lim, D. S.; Hui, D. *Ann. Eur. Acad. Sci.* **2003**, 314.
(7) Volodin, A.; Haesendonck, C. V.; Tarkiainen, R.; Ahlskog, M.; Fonseca, A.; Nagy, J. B. *Appl. Phys. A* **2001**, *72*, S75.
(8) Volodin, A.; Ahlskog, M.; Seynaeve, E.; Haesendonck, C. V.; Fonseca, A.; Nagy, J. B. *Phys. Rev. Lett.* **2000**, *84*, 3342.
(9) Wen, Y. K.; Shen, Z. M. *Carbon* **2001**, *39*, 2369.
(10) Ivanov, V.; Nagy, J. B.; Lambin, Ph.; Lucas, A.; Zhang, X. B.; Zhang, X. F.; Bernaerts, D.; Tendeloo, G. V.; Amelinckx, S.; Landuyt, J. V. *Chem. Phys. Lett.* **1994**, *223*, 329.
(11) Hernadi, K.; Thien-Nga, L.; Forro, L. *J. Phys. Chem. B* **2001**, *105*, 12464.
(12) Motojima, S.; Hasegawa, I.; Kagiya, S.; Andoh, K.; Iwanag, H. *Carbon* **1995**, *33*, 1167.
(13) Forzatti, P.; Lietti, L. *Catal. Today* **1999**, *52*, 165.
(14) Fonseca, A.; Hernadi, K.; Nagy, J. B.; Lambin, Ph.; Lucas, A. A. *Synth. Met.* **1996**, *77*, 235.
(15) Fonseca, A.; Hernadi, K.; Nagy, J. B.; Lambin, Ph.; Lucas, A. A. *Carbon* **1995**, *33*, 1759.
(16) Dunlop, B. I. *Phys. Rev. B* **1994**, *49*, 5643.
(17) Ou-Yang, Z. C.; Su, Z. B.; Wang, C. L. *Phys. Rev. Lett.* **1997**, *78*, 4055.
(18) Motojima, S.; Chen, Q. Q. *J. Appl. Phys.* **1999**, *85*, 3919.
(19) Iijima, S.; Ichihashi, T.; Ando, Y. *Nature* **1992**, *356*, 776.
(20) Kroto, H. W.; Mckay, K. *Nature* **1988**, *331*, 328.
(21) Terrones, H.; Terrones, M.; Hemandez, E.; Grobert, N.; Charlier, J. C.; Ajayan, P. M. *Phys. Rev. Lett.* **2000**, *84*, 1716.
(22) Biro, L. P.; Ehlich, R.; Khanh, N. Q.; Vertesy, Z.; Osvath, Z.; Koos, A.; Horvath, Z. E.; Gyulai, J.; Nagy, J. B. *Mater. Sci. Eng. C* **2002**, *19*, 3.